



# PCCP

**Extended Hamiltonian molecular dynamics: Semiclassical trajectories with improved maintenance of zero point energy**

Journal:	<i>Physical Chemistry Chemical Physics</i>
Manuscript ID	CP-ART-08-2018-004914.R2
Article Type:	Paper
Date Submitted by the Author:	24-Oct-2018
Complete List of Authors:	Shu, Yanan; University of Minnesota, Chemistry Dong, Sijia; University of Minnesota College of Science and Engineering, Chemistry Parker, Kelsey; University of Minnesota, Chemistry Bao, Junwei; University of Minnesota, Chemistry Zhang, Linyao; University of Minnesota Truhlar, Donald; Department of Chemistry, University of Minnesota

SCHOLARONE™  
Manuscripts

## Extended Hamiltonian molecular dynamics: Semiclassical trajectories with improved maintenance of zero point energy<sup>†</sup>

Yinan Shu, Sijia S. Dong, Kelsey A. Parker, Junwei L. Bao, Linyao Zhang, and Donald G. Truhlar\*

*Department of Chemistry, Chemical Theory Center, and Minnesota Supercomputing Institute, University of Minnesota, Minneapolis, Minnesota 55455-0431, United States*

**ABSTRACT:** It is well known that classical trajectories, even if they are initiated with zero point energy (ZPE) in each mode (trajectories initiated this way are commonly called quasiclassical trajectories) do not maintain ZPE in the final states. The energy of high-frequency modes will typically leak into low-frequency modes or relative translation of subsystems during the time evolution. This can lead to severe problems such as unphysical dissociation of a molecule, production of energetically disallowed reaction products, and unphysical product energy distributions. Here a new molecular dynamics method called extended Hamiltonian molecular dynamics (EHMD) is developed to improve the ZPE problem in classical molecular dynamics. In EHMD, two images of a trajectory are connected by one or more springs. The EHMD method is tested with the Henon-Heiles Hamiltonian in reduced and real units and with a Hamiltonian with quartic anharmonicity in real units, and the method is found to improve zero-point maintenance as intended.

**KEYWORDS:** anharmonicity, Henon-Heiles Hamiltonian, molecular dynamics, quasiclassical trajectory, vibrational energy, zero point energy

<sup>†</sup> Electronic supplementary information (ESI) available: It contains three more figures for cases A4 and C4. For ESI see DOI: [10.1039/c0000000000](https://doi.org/10.1039/c0000000000)

\* Corresponding author e-mail address: [truhlar@umn.edu](mailto:truhlar@umn.edu)

Advances in theoretical methods and computational power have made molecular dynamics (MD) simulations a powerful tool to investigate physical and chemical processes. Among various MD methods, classical trajectories and quasiclassical trajectories (which are classical trajectories with quantum mechanical selection of initial conditions) stand out as the most popular.<sup>1,2,3,4,5,6,7,8,9,10,11,12</sup> Despite the success of these methods, the use of classical trajectories suffers from two major problems, namely neglect of tunneling and failure to enforce the requirement of zero point energy (ZPE). To alleviate these problems, various semiclassical methods have been suggested, but these methods raise the cost and complexity of the calculations and sometimes have other limitations, for example they may be limited to simulating thermally averaged ensembles. Therefore, it is worthwhile to look for a simpler scheme that requires minimal changes to conventional classical trajectory propagation. In recent work we have shown how to include tunneling in classical trajectories.<sup>13</sup> Here we present a proposal to alleviate the ZPE problem.

The ZPE problem studied here is the phenomenon that in classical trajectories on anharmonic systems (and all real molecules are anharmonic), the high-frequency modes leak energies into the low-frequency modes or relative translation of fragments without the constraint of the quantum mechanical effect that the ZPE is the lowest allowed energy in a vibrational mode. The partition of ZPE into individual modes is not unique except for systems with no rotation and a quadratic (i.e., harmonic) vibrational potential; nevertheless most molecules have small enough anharmonicity that a harmonic calculation of the energy in a given mode should not yield an energy significantly below the harmonic zero point energy. Thus the dynamics of an isolated molecule should maintain ZPE in each mode to within the accuracy of the harmonic approximation. However, it is well known that classical mechanics does not maintain the ZPE in each mode. Strictly speaking, ZPE is required only for stationary states, such as the reactants and products of a chemical reaction, but it is reasonable to expect ZPE to be approximately maintained in spectator modes, and we know that approximate ZPE maintenance is important even in active modes at transition states.<sup>14,15,16,17</sup> Furthermore, the simulation of reactions by classical mechanics may produce species whose total vibrational energy is less than the total ZPE; in such a case, reactions may occur at energies that are energetically forbidden according to quantum mechanics. Such unphysical behavior of classical trajectories can also cause spurious

energy transfer or artificial dissociation of a molecular system. These problems have been well studied.<sup>18,19,20,21,22,23,24,25,26</sup> The ZPE problem originates from the fact that the classical trajectories can enter regions of the phase space that correspond to energy distributions not allowed by quantum mechanics.<sup>27,28,29</sup>

Many strategies have been proposed to tackle the ZPE problem of classical trajectories. These strategies can be generally classified into three types: (i) active methods, in which individual trajectories or ensemble behaviors are altered such that the regions of the phase space forbidden by QM are avoided in classical trajectories.<sup>30,31,32,33,34,35,36,37,38,39,40</sup> (ii) passive methods, in which unphysical trajectories are simply discarded from the final statistics.<sup>19,41,42,43,44,45,46,47,48</sup> (iii) methods that incorporate quantum mechanical effects in trajectories, for example, path-integral-based MD schemes,<sup>11,49,50,51,52,53,54,55,56,57</sup> Bohmian dynamics,<sup>58</sup> and other semiclassical dynamics schemes.<sup>59,60,61,62,63</sup> Most of these methods deal with individual trajectories, although from one point of view ZPE maintenance is the property of an ensemble of trajectories.<sup>28,29</sup> A disadvantage of active methods is that they may have drastic effects on the time evolution of the classical trajectories.<sup>32,36,37</sup>

Here we present a simple and computationally efficient ansatz that reduces the ZPE problem in classical trajectories. We call this new method extended Hamiltonian molecular dynamics (EHMD). The EHMD method maintains the simplicity of classical trajectories as much as possible. The goal of EHMD is not to achieve accurate quantum results, but rather to define semiclassical trajectories whose mode energies behave more quantum mechanically than those in purely classical trajectories, and thus to enable more realistic classical-like simulations of problems where the ZPE problem is a significant detriment to the ability of classical or quasiclassical simulations to interpret experimental results.

**Extended Hamiltonian.** Consider a system with  $F$  vibrational degrees of freedom. Here we treat all degrees of freedom semiclassically; extensions to many-body Hamiltonians including translation and rotation and where some coordinates are treated semiclassically and others classically are possible but are relegated to possible later work. We use isoinertial coordinates with all masses scaled to a reduced mass of  $\mu$ . Then the Hamiltonian is

$$H = \frac{1}{2m} \sum_{m=1}^F \dot{p}_m^2 + V(q_1, \dots, q_F) \quad (1)$$

where  $q_i$  is a vibrational coordinate, and  $p_i$  is its conjugate momentum. The extended Hamiltonian is then

$$H_{\text{ext}} = \sum_{g=1}^2 \left[ \frac{1}{2m} \sum_{m=1}^F \left( p_m^{(g)} \right)^2 + V \left( q_1^{(g)}, \dots, q_F^{(g)} \right) \right] + \frac{1}{2} \sum_{m=1}^F k_m \left( q_m^{(1)} - q_m^{(2)} \right)^2 \quad (2)$$

where  $k_m$  is a user-defined spring constant. The first sum represents two images of a trajectory, and if the spring constants were zero, these would just be two independent trajectories. The second sum in eq 2 couples the images. The equations of motion for EHMD are purely classical, i.e.,

$$\dot{p}_m^{(\gamma)} = - \frac{\partial H_{\text{ext}}(p_1^{(1)}, \dots, q_m^{(2)})}{\partial q_m^{(\gamma)}} \quad (3)$$

$$\dot{q}_m^{(\gamma)} = \frac{\partial H_{\text{ext}}(p_1^{(1)}, \dots, q_m^{(2)})}{\partial p_m^{(\gamma)}} \quad (4)$$

*The Henon-Heiles Hamiltonian.* First we use the Henon-Heiles system to illustrate the behavior of EHMD because the Henon-Heiles system of two coupled oscillators<sup>64,65</sup> ( $F = 2$ ) has been widely employed to investigate the ZPE problem in classical MD.<sup>28,30,32,36,37,66</sup> The Henon-Heiles Hamiltonian is given by eq 1 with

$$V(q_1, \dots, q_F) = \frac{1}{2} k_1 q_1^2 + \frac{1}{2} k_2 q_2^2 + \lambda \left( q_1^2 q_2 - \frac{1}{3} q_2^3 \right) \quad (5)$$

where

$$k_m = m \omega_m^2 \quad (6)$$

and  $\omega_m$  is the vibrational frequency in radians/s. The frequencies in radians/s are related to the frequencies  $\nu_m$  in wave numbers by  $\omega_m = 2\pi c \nu_m$ , where  $c$  is the speed of light.

In the present work, the initial conditions for an ensemble of trajectories are selected by random sampling of the harmonic part of the Hamiltonian. To be more specific, we assign a random number from a uniform distribution in the interval  $(0, 2\pi)$  to each vibrational phase  $\phi_m^{(g)}$  and assign the momenta and coordinates by

$$p_m^{(\gamma)} = \sqrt{(2n_m + 1)\hbar\mu\omega_m} \sin \phi_m^{(\gamma)} \quad (8a)$$

$$q_m^{(\gamma)} = \sqrt{(2n_m + 1)\hbar / (\mu\omega_m)} \cos \phi_m^{(\gamma)} \quad (8b)$$

where  $n_m$  is the vibrational quantum number. The mode energies along the trajectory are functions of time defined harmonically as

$$E_m^{(g)} = \frac{1}{2m} \left( p_m^{(g)} \right)^2 + \frac{1}{2} m \omega_m^2 \left( q_m^{(g)} \right)^2 \quad (9)$$

where the justification for using harmonic energies to monitor ZPEs was discussed in the introduction. We will consider two kinds of cases, first using the reduced units in which the Henon-Heiles system is usually studied and then using real units to make a connection with realistic levels of anharmonicity for real molecules. The reduced units are widely employed in previous work and hence provide a touchstone to connect to that work. The modeling results with real units will show how EHMD behaves for systems with realistic molecular parameters. For example, the Henon-Heiles model Hamiltonian can be employed to approximate the vibrations of linear CO<sub>2</sub>.<sup>67</sup>

An ensemble of 500 trajectories was computed for each case with  $n_1 = n_2 = 0$ , which means the harmonic energy of each mode equals the harmonic ZPE at the beginning of the trajectory. For EHMD, the mode energies are computed as the average of the two images, and the ensemble averages are therefore averages over 1000 images.

**Examples in reduced units.** In the reduced unit case,  $m = 1$  and  $\hbar = 0.06$ . The mode energies as functions of time are shown in Figure 1. The first two systems considered here correspond to (a)  $\omega_1 = \omega_2 = l = 1$  and (b)  $\omega_1 = 1.7, \omega_2 = 1, l = 1.5$ . System (a) is a case that has been studied in previous work.<sup>28,32</sup> For EHMD, we set  $k_1 = k_2 = 0.1$  for system (a) and  $k_1 = 0.34, k_2 = 0.15$  for system (b). The mode energies of the EHMD and classical MD results are shown in Figure 1.

In Figure 1(a), the modes have the same frequency; hence both modes have the same energy at the beginning of the trajectory. The classical MD mode energies show large energy flows between the modes, and the two mode energies end up differing by about 0.004 energy units after 500 time units. The EHMD mode energies are more stable than the classical ones, and – although we still see some level of ZPE leaking between the two modes – we do not see one mode losing a large amount of energy to the other. The EHMD results are much better than the passive methods

reported before,<sup>28</sup> and they are comparable to the active method.<sup>32</sup>

Figure 1(b) shows an example where two modes have different frequencies. The mode energies start with ZPEs of 0.051 and 0.030. In about 200 reduced time units, the two mode energies of the classical simulation become very close to 0.041, which indicates a significant ZPE leakage from the high-frequency mode to the low-frequency mode. In contrast, in EHMD, although the two mode energies change rapidly at the beginning, they are stabilized after 100 time units, and they become close to 0.046 and 0.037 for modes 1 and 2 respectively. Thus at 500 time units the high-frequency mode has still not become classically equilibrated to the low-frequency one. Since the ratio of energy in the two modes stabilizes, it is possible that one could improve the results even further by devising a better way to select the initial conditions of the ensemble, but we do not pursue that here.

In Figure 1(c), we show an example corresponding to Fermi resonance, where the ratio of the frequencies is 2:1; in particular we have  $\omega_1 = 2.0$ ,  $\omega_2 = 1$ ,  $\lambda = 1$ . The initial mode energies are 0.06 and 0.03. Classical MD results clearly show energy flow from the high-frequency mode to the low-frequency mode, and the two mode energies become nearly the same in about 400 time units; EHMD shows some leak from the high-frequency mode to the low-frequency mode in about 50 time units, but the mode energies are stable after that.

Thus the EHMD method is a significant improvement over classical MD in all three cases.

**Examples with cubic anharmonicity and real units.** We next consider three systems with realistic units based roughly on real systems: (A3) a system with frequencies equal to the asymmetric and symmetric stretching modes of CO<sub>2</sub> with frequencies,  $\nu_1 = 2565 \text{ cm}^{-1}$  and  $\nu_2 = 1480 \text{ cm}^{-1}$  (1  $\text{cm}^{-1}$  corresponds to 11.96 J/mol); (B3) a system with frequencies equal to the H<sub>2</sub>O symmetric and asymmetric stretching modes with frequencies  $\nu_1 = 3585 \text{ cm}^{-1}$  and  $\nu_2 = 3506 \text{ cm}^{-1}$ ; and (C3) a system with frequencies equal to the H<sub>2</sub>O symmetric stretch and bending frequencies,  $\nu_1 = 3585 \text{ cm}^{-1}$  and  $\nu_2 = 1885 \text{ cm}^{-1}$ . We set  $\mu$  equal to the reduced mass of CO for case A and to the reduced mass of OH for systems B and C. The numerical value of the anharmonic constant  $\lambda$  is set to  $0.5(k_1 + k_2)/a_0$  (where  $a_0$  is a bohr; 1  $a_0 = 0.5292 \times 10^{-10} \text{ m}$ ) in cases A3 and B3, which is a reasonable approximation to a higher-order force constant for the bond stretching modes.<sup>68,69</sup> For system C3, we set  $\lambda$  equal to  $0.25(k_1 + k_2)/a_0$ . The spring constants  $\kappa$  for the EHMD calculations are (in the usual units of mdyne/Å, where 1 mdyne/Å = 1 N/cm): (A3)  $\kappa_1 = 1.713$ ,  $\kappa_2$

= 2.911, (B3)  $\kappa_1 = \kappa_2 = 0.623$ , (C3)  $\kappa_1 = 0.4050$ ,  $\kappa_2 = 0.7784$ .

Parts (a), (c), and (e) of Figure 2 show the classical MD mode energies as functions of time in red and blue and the EHMD mode energies as functions of time in yellow and green for systems A3, B3, and C3, respectively. The figures show that EHMD preserves ZPE much better than classical MD. The EHMD mode energies are stabilized after  $\sim 200$  fs in all three systems. However, in classical MD, we can see a strong oscillatory energy flow between the two modes during the whole simulation time for systems A and B. For system C, the two mode energies become very close to each other after 300 fs.

To obtain a better quantitative understanding of the differences between the trajectories of classical MD and EHMD, we computed the histogram of mode energy distribution along the trajectories, and these are shown in Figs. 2(b), 2(d), and 2(f). One can see that, in all cases, the mode energy distribution for EHMD is much narrower than classical MD. We do see some ZPE leaking from the most probable mode energies in EHMD; however, the leakage is much smaller than in classical MD.

At the present time, we have not determined the optimum way to set the  $\kappa_m$  values. In our experience, the quality of the trajectory results is not overly sensitive to the  $\kappa_m$  values, by which we mean that the ensemble-averaged mode energies are stable within certain ranges of  $\kappa$  values. However, the best results are usually obtained with  $\kappa$  values that are about 10 to 20 percent of the quadratic force constant of the target mode. Here target mode means the mode into which the energy is leaking. All force constants used for Figure 2 are given in the Table 1, which shows that the three values of  $\kappa_1/k_2$  are all in the range 9–21%, and the three values of  $\kappa_2/k_1$  are all in the range 9–11%. Figure 3 shows an example for system A with three other sets of  $\kappa_m$  values, which differ by as much as 29% from those in in Figure 2(a); all the EHMD results show very similar behavior.

Table 1. The quadratic force constants  $k_1$  and  $k_2$  in units of  $\text{N cm}^{-1}$ , the cubic anharmonicity parameter  $\lambda$  in units of  $\text{N cm}^{-1} \text{ \AA}^{-1}$ , and the spring constants  $\kappa$  in units of  $\text{N cm}^{-1}$ .

System	A3	B3	C3
$k_1$	26.581	7.128	7.128
$k_2$	8.850	6.818	1.971
$\lambda$	33.478	13.177	4.299
$\kappa_1$	1.713	0.623	0.4050
$\kappa_2$	2.991	0.623	0.7784

Note that  $1 \text{ N/cm}$  is the same as the conventional force constant unit of  $1 \text{ mdyn/\AA}$ , and  $1 \text{ N cm}^{-1} \text{ \AA}^{-1}$  is the same as  $1 \text{ mdyn/\AA}^2$ .

**Test for a Hamiltonian with quartic anharmonicity.** To further demonstrate the generality of our method, we have also tested a system with quartic anharmonicity. The Hamiltonian is given by eq 1 with the following potential

$$V(q_1, \dots, q_F) = \frac{1}{2}k_1q_1^2 + \frac{1}{2}k_2q_2^2 + \lambda(q_1 - q_2)^4 \quad (10)$$

where  $k_m$  is defined in eq 6, and  $q_m$  is defined in eq 8. As examples, we considered systems like A3 and C3 that were tested with the Henon-Heiles Hamiltonian with real units. For both new systems, which will be called A4 and C4, the reduced mass and frequencies are defined in the same way as the real-unit examples for the Henon-Heiles Hamiltonian. The anharmonic constant  $\lambda$  is set to be  $l(k_1 + k_2)/a_0^2$ , where  $l$  is a parameter to be varied to see the effect on the results. The numerical values of the force constants are summarized in Table 2.

Table 2. The quadratic force constants  $k_1$  and  $k_2$  in units of  $\text{N cm}^{-1}$ , the quartic anharmonicity parameter  $\lambda$  in units of  $\text{N cm}^{-1} \text{ \AA}^{-2}$ , and the spring constants  $\kappa$  in units of  $\text{N cm}^{-1}$ .<sup>a</sup>

System	A4	C4
$k_1$	26.772	7.178
$k_2$	8.913	1.985
$\lambda$	63.717, <sup>b</sup> 127.434 <sup>c</sup>	8.180d, <sup>d</sup> 16.360 <sup>b</sup>
$\kappa_1$	2.335	0.1479
$\kappa_2$	0.7784	0.07784

<sup>a</sup> Note that  $1 \text{ N/cm}$  is the same as the conventional force constant unit of  $1 \text{ mdyn/\AA}$ , and  $1 \text{ N cm}^{-1} \text{ \AA}^{-2}$  is the same as  $1 \text{ mdyn/\AA}^3$ . <sup>b</sup>  $l = 0.5$  <sup>c</sup>  $l = 1$  <sup>d</sup>  $l = 0.25$

Figure 4 compares the classical and EHMD mode energies of system A4 ( $l = 0.5, 1.0$ ) and

system C4 ( $l = 0.25, 0.5$ ). As we can see from Figure 4, regardless of the choice of  $\lambda$ , the mode energies of the classical trajectories are more spread-out than those for EHMD, and the mode energies from EHMD are much more stable. Different choices of  $\kappa_m$  values have also been explored. Figures S1-S3 in the Electronic Supplementary Information (ESI) show that for each choice of the anharmonic constant  $\lambda$ , EHMD with a wide range of  $\kappa_m$  values can maintain the zero-point energy much better than classical MD. For system A4, for both  $\lambda = 0.5(k_1 + k_2)/a_0^2$  and  $\lambda = (k_1 + k_2)/a_0^2$ , the EHMD mode energies are stable for  $\kappa_m/k_1$  in the range 9–61% and for  $\kappa_m/k_2$  in the range 3–20%. For system C4, for  $\lambda = 0.25(k_1 + k_2)/a_0^2$ ,  $\lambda = 0.5(k_1 + k_2)/a_0^2$ , and  $\lambda = (k_1 + k_2)/a_0^2$ , the EHMD mode energies are stable for  $\kappa_1/k_1$  in the range 2–42% and  $\kappa_2/k_2$  in the range 4–80%. (For brevity, values outside these ranges are not discussed here.) From Figures S1 and S2, we notice that, if  $k_1/k_2 > 1$ , EHMD achieves better performance when  $\kappa_1/\kappa_2 > 1$ . These examples demonstrate that EHMD also works well for a system with quartic anharmonicity, and the result is robust with a wide range of force constants.

**Discussion.** The extended Hamiltonian is not designed to yield accurate quantum mechanical results, but rather to reduce the problem of ZPE leakage in the simplest possible way. The form of the spring term is motivated by the presence of harmonic springs in ring polymer MD (RPMD)<sup>55,56</sup> and by the linearized quantum force term in Bohmian dynamics with approximated quantum force (BD-AQP).<sup>58,70</sup> These two simulation approximations have common elements, and our work has similar elements, in particular the use of coupled trajectories to simulate the effect of the nonlocality of a quantum mechanical wave packet, but we have attempted to use these elements in a simpler way – by coupling only two trajectories. The RPMD equations involve all trajectories in a cyclic chain while the Bohmian approach developed by Garashchuk et al. connects all the trajectories to an averaged trajectory. In both cases, the individual trajectories experience a force from the other trajectories that can pull them closer together or push them further apart. The same is true for EHMD. Note that in EHMD, the restoring force of the spring ensures that the trajectories continue to remain close and affect one another. The comparison between RPMD, BD-AQP, and EHMD is schematically illustrated in Figure 5. Both RPMD and BD-AQP have had success in reducing ZPE leakage. Specifically, Habershon and Manolopoulos have shown that RPMD conserves ZPE for inter- and intramolecular modes of a water model better than the linearized semiclassical initial value

representation,<sup>52</sup> and Garashchuk and Rassolov have shown BD-AQP conserves ZPE in a one-dimensional Morse oscillator as well as in modified multi-dimensional oscillators.<sup>58</sup> We emphasize the following important differences between EHMD and these methods: (i) The  $\kappa$  parameter in the EHMD extended term is not temperature dependent as in RPMD. (ii) The extended term (the potential energy in the springs) is associated with the difference of the coordinates in two trajectories, while in BD-AQP, the quantum force term is derived using a set of trajectories. (iii) EHMD is designed to be simpler than either of the more rigorous semiclassical methods, and the amount of work simply doubles, whereas it can go up by a large factor in the other methods.

Another aspect of the similarity of the present method to a previous semiclassical method is the analogy to the displaced point path integral method,<sup>71,72</sup> here we have displaced trajectories rather than displaced points.

The strictly conserved energy in the extended Hamiltonian is the sum of the energies of two images plus the energy of the extended term. One can ask whether we see strong energy transfer between the extended term and the individual images. Figure 6 shows energies in the two springs and their sum for the A, B, and C systems with cubic anharmonicity with real units (Henon-Heiles systems of Figure 2). One can see that spring energies are roughly 10%-20% of the mode energies, and they are conserved very well during the time propagation. This indicates that although the energies of the individual images are not strictly conserved, they are approximately conserved very well in an average sense.

We have interpreted the energies of the trajectories as being the energies of the images excluding the spring potentials. An alternative interpretation is shown in Figure 7, where we added half of each spring's potential energy into each of the two modes that are coupled by the spring. We can call the sums the augmented mode energies. Figure 7 shows the augmented mode energies the cubic A, B, and C systems of Figure 2. One sees the augmented mode energies are all shifted up for the EHMD, because we included the potential energy of the extended term here. This extra energy has similar behavior as in BD-AQP, where the quantum mechanical Gaussian will add some extra energy to the system. The augmented mode energies are much better conserved than the mode energies of classical MD.

In this article, we have presented a new semiclassical molecular dynamics method, called

---

extended Hamiltonian molecular dynamics. The EHMD method is designed to improve the treatment of the ZPE in classical trajectories. In the extended Hamiltonian ansatz, a trajectory has two images coupled by springs. By employing the Henon-Heiles Hamiltonian as well as Hamiltonian with a quartic potential as test systems, we have shown that EHMD maintains ZPE much better than classical MD in eight test cases. Extensions and improvements are possible, but this work demonstrates the possibility to improve classical trajectory simulations in a very simple way.

#### ACKNOWLEDGMENTS

The authors are grateful to Sophya Garashchuk for helpful discussions. This work was supported in part by the U.S. Department of Energy, Office of Science, Office of Basic Energy Sciences under award number DE-SC0015997. The authors declare no competing financial interest.

#### ORCID

Yinan Shu: 0000-0002-8371-0221

Kelsey A. Parker: 0000-0002-9176-3681

Junwei Lucas Bao: 0000-0002-4967-663X

Sijia S. Dong: 0000-0001-8182-6522

Linyao Zhang: 0000-0003-1848-8860

Donald G. Truhlar: 0000-0002-7742-7294

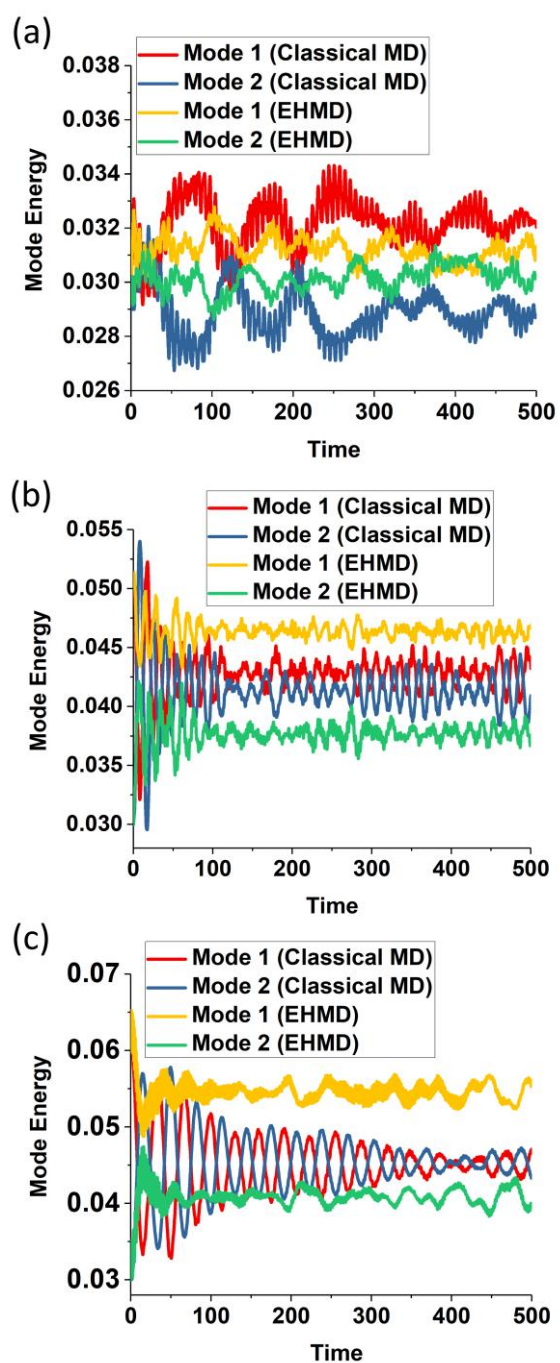


**Figure 1.** The two mode energies as a function of time are shown as red, blue colors for classical MD and yellow, green colors for EHMD (Henon-Heiles Hamiltonian). The two conditions are, (a)  $\omega_x = \omega_y = 1$ , (b)  $\omega_x = 1.7, \omega_y = 1$ , (c)  $\omega_x = 2.0, \omega_y = 1$

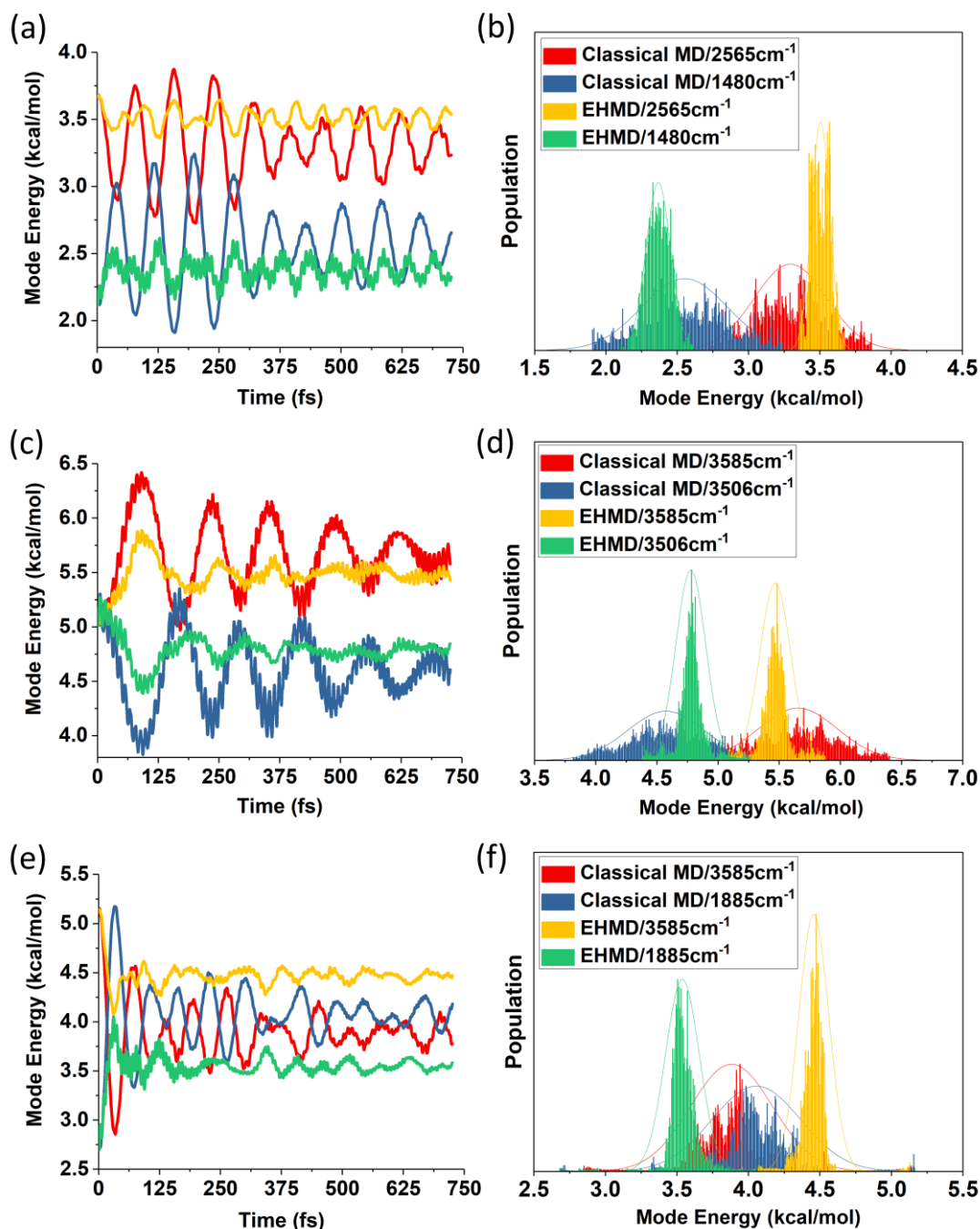


**Figure 2.** In plots (a), (c), and (e), the mode energies as functions of time are shown in red and blue for classical MD and in yellow and green for EHMD (Henon-Heiles Hamiltonian). Plots (b), (d), and (f) give histograms of mode energies distribution for classical MD and EHMD. The same colors are used as in panels (a), (c) and (e). The top, middle, and bottom pairs of plots correspond respectively to systems A3, B3, and C3.

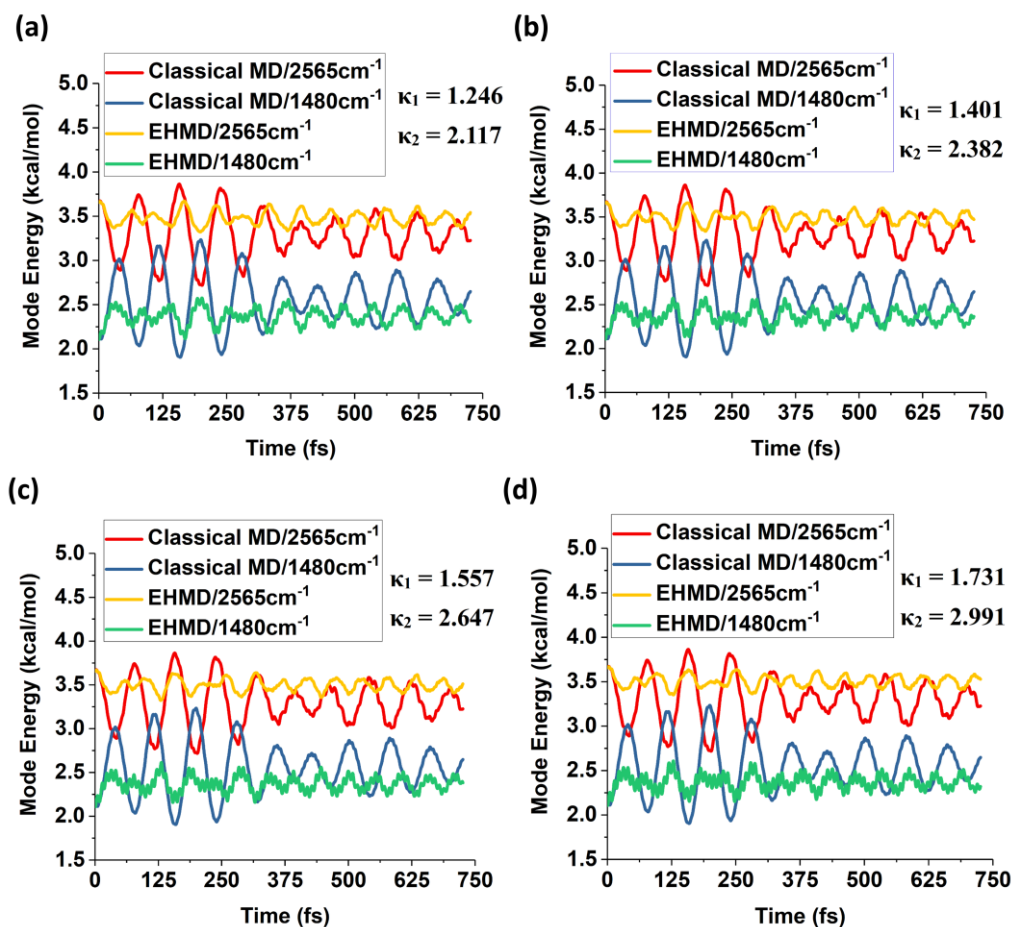


**Figure 3.** The classical and EHMD (Henon-Heiles Hamiltonian) mode energies as functions of time for system A with different  $\kappa$  parameters. This shows that the EHMD results are stable within a range of  $\kappa$  parameters. The classical mode energies are shown in red and blue, and the EHMD mode energies are shown in yellow and green. Four sets of  $\kappa$  parameters are shown: (a)  $\kappa_1 = 1.246$ ,  $\kappa_2 = 2.117$ ; (b)  $\kappa_1 = 1.401$ ,  $\kappa_2 = 2.382$ ; (c)  $\kappa_1 = 1.557$ ,  $\kappa_2 = 2.647$ ; and (d)  $\kappa_1 = 1.731$ ,  $\kappa_2 = 2.991$ , where the force constants are in N/cm (same as mdyne/Å). Notice that panel (d) is the same as Fig. 2(a).

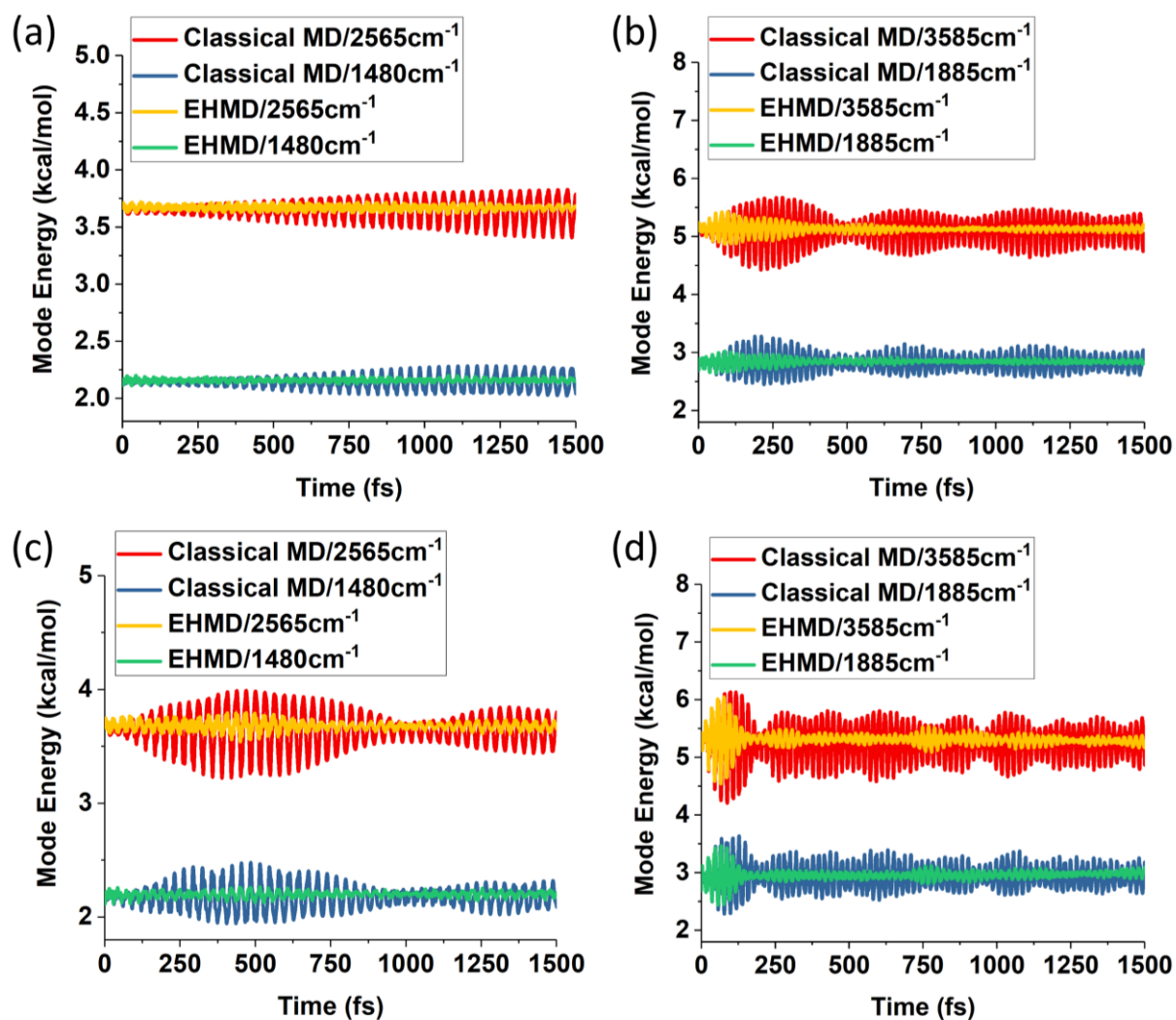


**Figure 4.** Comparison of the classical MD and EHMD with quartic anharmonicity for: (a) and (c): quartic system A4; and (b) and (d): quartic system C4. The mode energies as functions of time are shown in red and blue for classical MD and in yellow and green for EHMD. (a)  $l = 0.5$ , (b)  $l = 0.25$ , (c)  $l = 1.0$ , (d)  $l = 0.5$ .

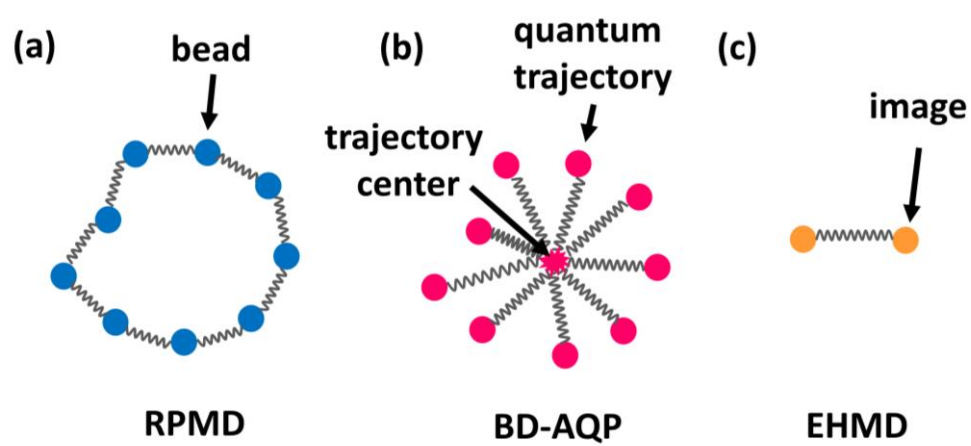


**Figure 5.** The conceptual illustration of the connected individual trajectories, in (a). RPMD, (b). BD-AQP, and (c). EHMD.

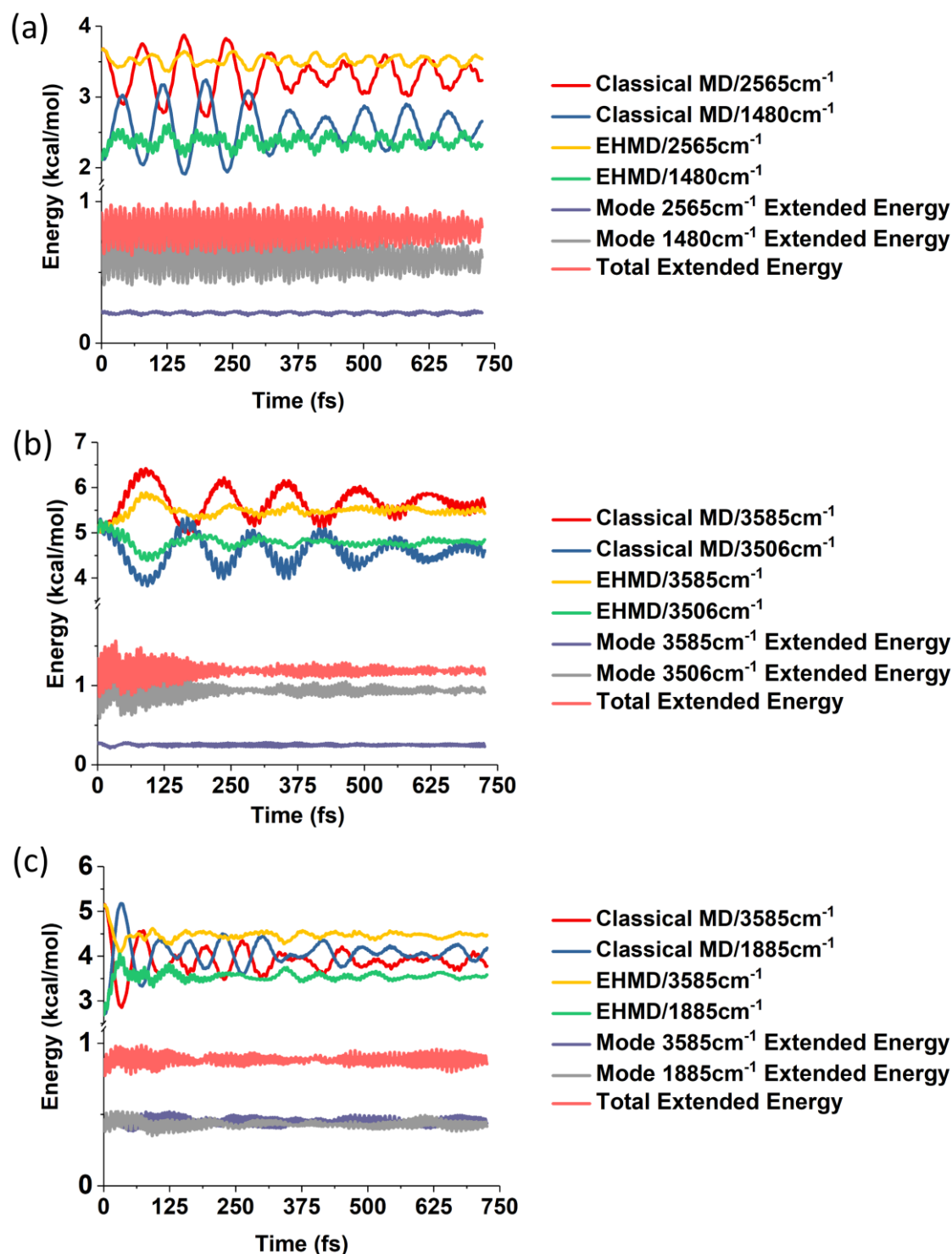


Figure 6. The classical MD and EHMD (Henon-Heiles Hamiltonian) mode energies and the extended-term energy as functions of time for systems A3, B3, and C3 of Figure 2. The classical MD mode energies are shown in red and blue; EHMD mode energies are shown in yellow and green. The separate spring potential energies for the two modes separately are shown in purple and grey, and the total energy of the extended term (sum of the two spring potential energies) is shown in vermilion.

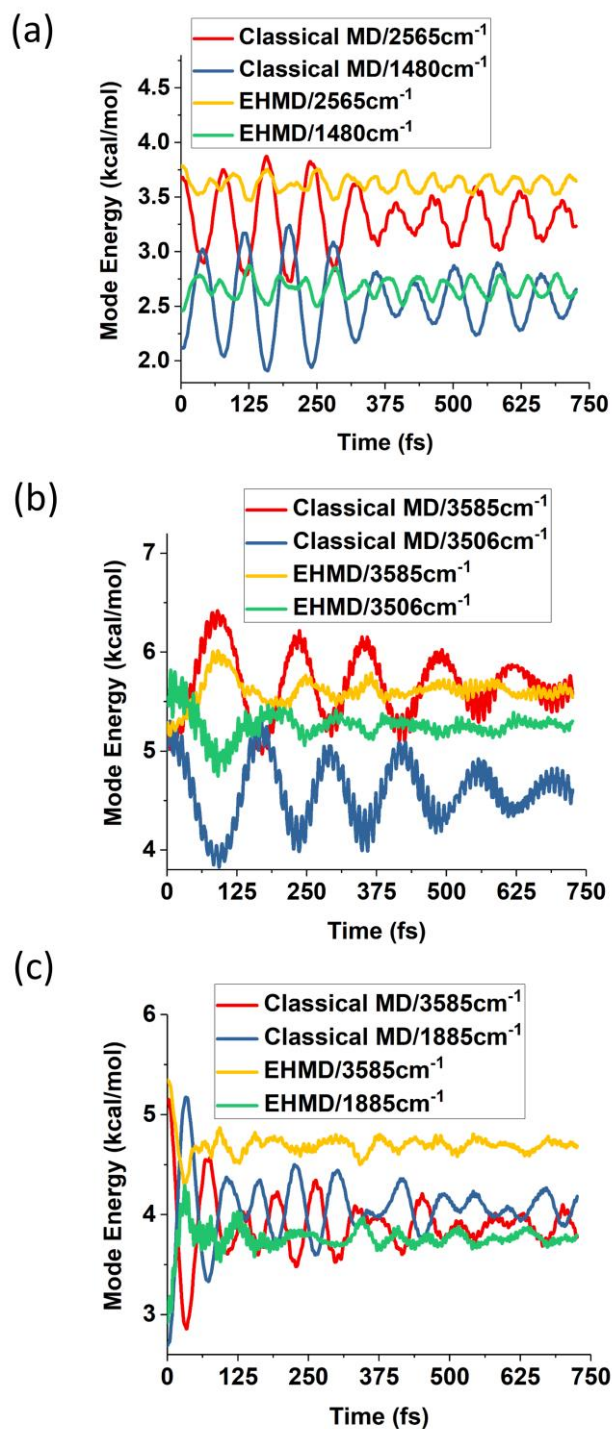


Figure 7. The classical and EHMD (Henon-Heiles Hamiltonian) mode energies as functions of time for systems A3, B3, and C3 defined in the text. Here the mode energies for EHMD are defined by including one half of the potential energy of the spring for that mode. That is the reason one sees the mode energy shifted up for EHMD.

---

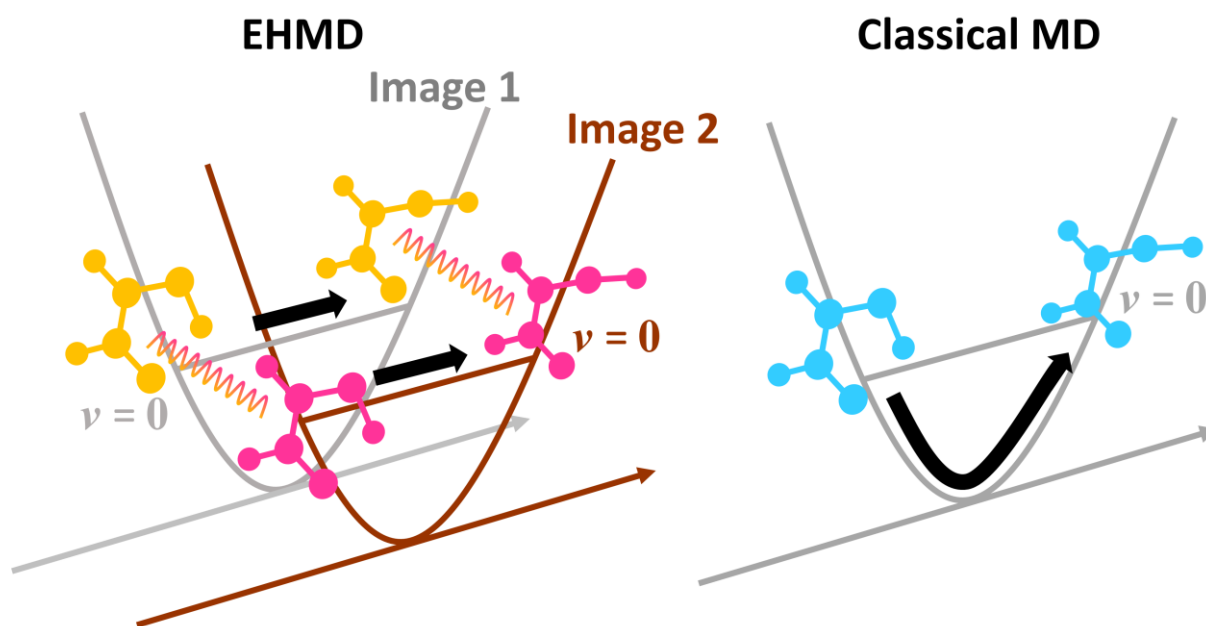
## References

- <sup>1</sup> F. Wall, I. Hiller and J. Mazur, *J. Chem. Phys.*, 1958, **29**, 255.
- <sup>2</sup> B. J. Alder and T. E. Wainwright, *J. Chem. Phys.*, 1959, **31**, 459.
- <sup>3</sup> D. L. Bunker, *Methods Comp. Phys.*, 1971, **10**, 287.
- <sup>4</sup> D. G. Truhlar and J. T. Muckerman, J. T. Reactive Scattering Cross Sections: Quasiclassical and Semiclassical Methods. In *Atom-Molecule Collision Theory: A Guide for the Experimentalist*, edited by R. B. Bernstein (Plenum Press, New York, 1979), p. 505.
- <sup>5</sup> L. M. Raff and D. L. Thompson, In *Theory of Chemical Reaction Dynamics*; M. Baer, Ed.; CRC Press: Boca Raton, 1985; Vol. 3, p. 1.
- <sup>6</sup> W. Van Gunsteren, In *Mathematical Frontiers in Computational Chemical Physics*; D. G. Truhlar, Ed.; Springer-Verlag: New York, 1988; p. 136.
- <sup>7</sup> M. P. Allen and D. J. Tildesley *Computer Simulation of Liquids*; Oxford University Press: New York, 1990.
- <sup>8</sup> G. C. Schatz, M. ter Horst and T. Takayanagi, In *Modern Methods for Multidimensional Dynamics Computations in Chemistry*; D. L. Thompson, Ed.; World Scientific: Singapore, 1998; p. 1.
- <sup>9</sup> P. A. Kollman, *Theor. Chem. Acc.*, 2000, **103**, 306.
- <sup>10</sup> D. Frenkel and B. Smit, *Understanding Molecular Simulation*; 2nd ed.; Academic Press: San Diego, 2002.
- <sup>11</sup> D. Marx and J. Hutter, *Ab Initio Molecular Dynamics*; Cambridge University Press: Cambridge, 2009.
- <sup>12</sup> M. Karplus, *Angew. Chem. Int. Ed.*, 2014, **53**, 9992.
- <sup>13</sup> J. Zheng, X. Xu, R. Meana-Pañeda and D. G. Truhlar, *Chem. Sci.*, 2014, **5**, 2091.
- <sup>14</sup> R. A. Marcus, *Discuss. Faraday Soc.*, 1976, **44**, 7.
- <sup>15</sup> D. G. Truhlar and A. D. Isaacson, *J. Chem. Phys.*, 1982, **77**, 3516.
- <sup>16</sup> K. Haug, D. W. Schwenke, Y. Shima, D. G. Truhlar, J. Zhang and D. J. Kouri, *J. Phys. Chem.*, 1986, **90**, 6757.
- <sup>17</sup> D. C. Chatfield, R. S. Friedman, D. W. Schwenke and D. G. Truhlar, *J. Phys. Chem.*, 1992, **96**, 2414.
- <sup>18</sup> J. M. Bowman and A. Kuppermann, *J. Chem. Phys.*, 1973, **59**, 6524.
- <sup>19</sup> J. C. Gray, D. G. Truhlar, L. Clemens, J. W. Duff, F. M. Chapman Jr, G. O. Morrell and E. F. Hayes, *J. Chem. Phys.*, 1978, **69**, 240.
- <sup>20</sup> W. L. Hase and D. G. Buckowski, *J. Comput. Chem.*, 1982, **3**, 335.
- <sup>21</sup> G. C. Schatz, *J. Chem. Phys.*, 1983, **79**, 5386.
- <sup>22</sup> L. L. Gibson, G. C. Schatz, M. A. Ratner and M. J. Davis, *J. Chem. Phys.*, 1987, **86**, 3263.
- <sup>23</sup> D. H. Lu, W. L. Hase, *J. Chem. Phys.*, 1988, **89**, 6723.
- <sup>24</sup> P. H. Nguyen and G. Stock, *J. Chem. Phys.*, 2003, **119**, 11350.
- <sup>25</sup> G. Stock, *Phys. Rev. Lett.*, 2009, **102**, 118301.
- <sup>26</sup> S. M. Park, P. H. Nguyen and G. Stock, *J. Chem. Phys.*, 2009, **131**, 184503.
- <sup>27</sup> E. J. Heller, *Phys. Rev. A*, 1987, **35**, 1360.
- <sup>28</sup> Y. Guo, D. L. Thompson and T. D. Sewell, *J. Chem. Phys.*, 1996, **104**, 576.

- 
- <sup>29</sup> G. Stock, U. Müller, *J. Chem. Phys.*, 1999, **111**, 65.
- <sup>30</sup> J. M. Bowman, B. Gazdy and Q. Sun, *J. Chem. Phys.*, 1989, **91**, 2859.
- <sup>31</sup> W. H. Miller, W. L. Hase and C. L. Darling, *J. Chem. Phys.*, 1989, **91**, 2863.
- <sup>32</sup> T. D. Sewell, D. L. Thompson, J. D. Gezelter and W. H. Miller, *Chem. Phys. Lett.*, 1992, **193**, 512.
- <sup>33</sup> A. J. C. Varandas and J. M. C. Marques, *J. Chem. Phys.*, 1994, **100**, 1908.
- <sup>34</sup> G. H. Peslherbe and W. L. Hase, *J. Chem. Phys.*, 1994, **100**, 1179.
- <sup>35</sup> M. Ben-Nun and R. D. Levine, *J. Chem. Phys.*, 1996, **105**, 8136.
- <sup>36</sup> D. A. McCormack and K. F. Lim, *J. Chem. Phys.*, 1997, **106**, 572.
- <sup>37</sup> Z. Xie and J. M. Bowman, *J. Phys. Chem. A*, 2006, **110**, 5446.
- <sup>38</sup> D. Bonhommeau and D. G. Truhlar, *J. Chem. Phys.*, 2008, **129**, 014302.
- <sup>39</sup> G. Czakó, A. L. Kaledin and J. M. Bowman, *J. Chem. Phys.*, 2010, **132**, 164103.
- <sup>40</sup> G. Czakó, A. L. Kaledin and J. M. Bowman, *Chem. Phys. Lett.*, 2010, **500**, 217.
- <sup>41</sup> L. A. M. Quintales, A. J. C. Varandas and J. M. Alvaríño, *J. Phys. Chem.*, 1988, **92**, 4552.
- <sup>42</sup> T. Uzer, B. D. MacDonald, Y. Guan and D. L. Thompson, *Chem. Phys. Lett.*, 1988, **152**, 405.
- <sup>43</sup> D. H. Lu and W. L. Hase, *J. Chem. Phys.*, 1989, **91**, 7490.
- <sup>44</sup> G. Nyman and J. A. Davidsson, *J. Chem. Phys.*, 1990, **92**, 2415.
- <sup>45</sup> A. J. C. Varandas, *J. Chem. Phys.*, 1993, **99**, 1076.
- <sup>46</sup> A. J. Marks, *J. Chem. Phys.*, 1998, **108**, 1438.
- <sup>47</sup> A. J. C. Varandas, *Chem. Phys. Lett.*, 2007, **439**, 386.
- <sup>48</sup> A. K. Paul and W. L. Hase, *J. Phys. Chem. A*, 2016, **120**, 372.
- <sup>49</sup> J. Cao and G. A. Voth, *J. Chem. Phys.*, 1994, **101**, 6168.
- <sup>50</sup> S. Jang and G. A. Voth, *J. Chem. Phys.*, 1999, **111**, 2371.
- <sup>51</sup> I. R. Craig and D. E. Manolopoulos, *J. Chem. Phys.*, 2004, **121**, 3368.
- <sup>52</sup> T. D. Hone, P. J. Rossky and G. A. Voth, *J. Chem. Phys.*, 2006, **124**, 154103.
- <sup>53</sup> S. Habershon and D. E. Manolopoulos, *J. Chem. Phys.*, 2009, **131**, 244518.
- <sup>54</sup> H. Dammak, Y. Chalopin, M. Laroche, M. Hayoun and J. J. Greffet, *Phys. Rev. Lett.*, 2009, **103**, 190601.
- <sup>55</sup> R. Pérez de Tudela, F. J. Aoiz, Y. V. Suleimanov and D. E. Manolopoulos, *J. Phys. Chem. Lett.*, 2012, **3**, 493.
- <sup>56</sup> S. Habershon, D. E. Manolopoulos, T. E. Markland and T. F. Miller III, *Annu. Rev. Phys. Chem.*, 2013, **64**, 387.
- <sup>57</sup> F. Briec, Y. Bronstein, H. Dammak, P. Depondt, F. Finocchi, and M. Hayoun, *J. Chem. Theory Comput.*, 2016, **12**, 5688.
- <sup>58</sup> S. Garashchuk and V. A. Rassolov, *J. Chem. Phys.*, 2008, **129**, 024109.
- <sup>59</sup> R. Alimi, A. García-Vela and R. B. Gerber, *J. Chem. Phys.*, 1992, **96**, 2034.
- <sup>60</sup> X. Sun and W. H. Miller, *J. Chem. Phys.*, 1997, **106**, 6346.
- <sup>61</sup> X. Sun, H. Wang and W. H. Miller, *J. Chem. Phys.*, 1998, **109**, 7064.
- <sup>62</sup> E. J. Heller, *J. Chem. Phys.*, 1975, **62**, 1544.
- <sup>63</sup> E. J. Heller, *J. Chem. Phys.*, 1981, **75**, 2923.

- <sup>64</sup> M. Hénon and C. Heiles, *A. J.*, 1964, **69**, 73.
- <sup>65</sup> M. J. Davis, E. B. Stechel and E. J. Heller, *Chem. Phys. Lett.*, 1980, **76**, 21.
- <sup>66</sup> K. F. Lim and D. A. McCormack, *J. Chem. Phys.*, 1995, **102**, 1705.
- <sup>67</sup> J. M. Bowman, *J. Chem. Phys.*, 1978, **68**, 608.
- <sup>68</sup> J. F. Gaw and N. C. Handy, *Chem. Phys. Lett.*, 1986, **128**, 182.
- <sup>69</sup> K. M. Kuhler, D. G. Truhlar and A. D. Isaacson, *J. Chem. Phys.*, 1996, **104**, 4664.
- <sup>70</sup> S. Garashchuk and V. A. Rassolov, *J. Chem. Phys.*, 2004, **120**, 1181.
- <sup>71</sup> S. L. Mielke and D. G. Truhlar, *J. Chem. Phys.*, 2001, **115**, 652.
- <sup>72</sup> S. Mielke, M. Dinpajoo, J. I. Siepmann and D. G. Truhlar, *J. Chem. Phys.*, 2013, **138**, 014110.

### Graphical abstract



We present a new semiclassical molecular dynamics method designed to improve the treatment of the zero-point energy in quasiclassical trajectories.